Influence of Material Damping Characteristics on the Seismic Behavior of Rockfill Dams

Seyyed Kazem Razavi[1], Kosar Hadidi[2] & Samuel Yniesta[1]
[1]*Department of Civil, Geological, and Mining Engineering, Polytechnique Montréal, Montréal, QC, Canada*
[2]*Department of Civil Engineering, University of Tabriz, Tabriz, Iran*

ABSTRACT
Multi-dimensional nonlinear ground response analyses are slowly becoming the norm in earthquake engineering practice. However, they require advanced cyclic models that can reproduce the soil's dynamic behavior with high accuracy. In this study, a nonlinear cyclic model, developed by combining and modifying the formulations of existing nonlinear cyclic models, is introduced. The model is capable of taking any desired damping and shear modulus reduction curve as input parameters. An example of simulation is presented in which a set of reference curves is used to perform a 2D dynamic analysis to study the seismic behavior of a rockfill dam. The simulations are also performed with input curves obtained from the Masing rules to investigate the effect of material damping characteristics and investigate the limitations of Masing-type models. Results indicate that the damping curves generated by the Masing rules produce lower amplification in PGA for strong earthquakes, because Masing rule induce higher damping at large strains. Using the Masing rules and attempting to modify the shear modulus reduction curves to generate damping curves closer to the reference curve resulted in softer material, which significantly reduced the PGA amplification in the dam.

1 INTRODUCTION

Several nonlinear cyclic models implemented in 2D and 3D geotechnical earthquake engineering commercial software (Itasca 2012, ABAQUS 2011), take a normalized modulus reduction curve and a maximum shear modulus as input parameters, and use a set of rules to define the unloading/reloading path, which typically abides Masing rules (Masing 1926). However, these models have been criticized for their shortcomings, including over-prediction of damping at high cyclic shear strains and under-prediction at low cyclic shear strains (Hashash et al. 2010, Numanoglu et al. 2018, Yniesta et al. 2017). To address this issue, some researchers (Dakoulas 2012, Razavi et al. 2021) have attempted to modify the normalized modulus reduction curve to achieve a more reasonable damping curve under the use of Masing rules. The curves obtained through this methodology are referred to as modified MD curves in the present study. Using these curves, Dakoulas (2012) analyzed an earth structure's seismic behavior to design the most critical elements of dams, such as concrete face slabs, while Razavi et al. (2021) studied the seismic performance of a new plastic concrete cutoff wall as a rehabilitation method for an earth-fill dam.
However, it is known that even modest changes in the modulus reduction curve can induce a significant change in the shear stress-shear strain curve of soils and a shear strength that is usually different than expected or desired (Hashash et al., 2010). Consequently, it is essential to evaluate the impact of such assumptions made using the modified MD curves on the seismic response of earth structures. The assessment should be done by using backbone and damping curves derived from experimental data, such as the curves introduced by Rollins et al. in (2020) for gravelly soils, referred to as reference curves in this study. It is also essential to ensure that the backbone curves obtained from reference curves reach the soil's shear strength at large strains to be considered valid.
Here, a nonlinear model is developed using a combination of existing nonlinear cyclic models and implemented in FLAC. The model can reproduce both modified MD curves and reference curves by choosing appropriate material properties, making it possible to analyze the effect of using different backbone and material damping characteristic curves on the seismic response of earth-fill dams.

2 A COMBINED-IMPROVED NONLINEAR CYCLIC MODEL

2.1 Maximum shear modulus at small strains

The definition of G_{max} can be expressed using the following equation (Richard et al. 1973).

$$G_{max} = P_a \times A \frac{(B-e)^2}{1+e} \left(\frac{\sigma_m}{P_a}\right)^r \quad [1]$$

Where e and σ_m are the void ratio and the mean effective stress, respectively. The parameters r, A, and B are material properties, and P_a refers to the atmospheric pressure.

2.2 Backbone Curve

The backbone curve used in the modified MD curves follows equation 2 (Konder and Zelasko, 1963), whereas the backbone curve employed in the reference curves adheres to equation 3 (Yee et al. 2013).

$$\tau = \frac{G_{max}\gamma}{1+\left(\frac{\gamma}{\gamma_r}\right)^{\alpha}} \quad [2]$$

$$\tau = \begin{cases} \frac{G_{max}\gamma}{1+\left(\frac{\gamma}{\gamma_r}\right)^{\alpha}} & \gamma \le \gamma_1 \\ \tau_1 + \frac{G_{\gamma 1}\gamma}{1+\left(\frac{\tau_{max}-\tau_1}{G_{\gamma 1}}\right)} & \gamma > \gamma_1 \end{cases} \quad [3]$$

Where, τ, γ, γ_r, and α are shear stress, shear strain, reference strain, and curve-fitting coefficient, respectively. τ_1 and $G_{\gamma 1}$ are the shear stress and shear modulus for $\gamma = \gamma_1$ obtained from equation 2. While taking α a constant value, γ_r varies with the variation of σ_m as well as soil parameters such as over consolidation ratio (OCR), plasticity index, PI, and the coefficient of uniformity, C_u. Rollins et al. (2020) proposed equation 4 to calculate γ_r for granular soils.

$$\gamma_r = 0.0046(C_u)^{-0.197}(\sigma_m)^{0.52} \quad [4]$$

τ_{max} in equation 3, is the shear strength of the soil and can be calculated using equation 5 for granular materials.

$$\tau_{max} = \sigma_m \sin(\phi) \quad [5]$$

Where ϕ is the friction angle. Equation 3 introduces a two-hyperbola backbone curve modifying the hyperbola curve of equation 2 to reach τ_{max} by passing γ from γ_1. Schematic form of the introduced backbone curves is shown in Figure 1. In this paper, γ_1 is the shear strain at which $\tau_1 = 0.75\tau_{max}$.

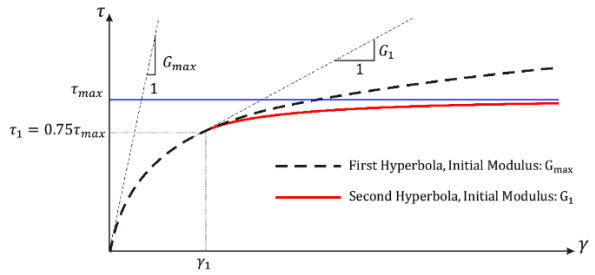

Figure 1 Using two hyperbola approach to modify the shear stress-shear strain curve at large strains in the backbone curve

Equation 3, which is utilized in the reference curves, ensures that the soil's shear strength at high strains is reached. In contrast, equation 2, employed in the modified MD curves, does not achieve this objective.

2.3 Damping curve

The shear modulus in the unloading/reloading denoted here as G_{NM} is obtained from equation 6. where subscript NM is the abbreviation for non-Masing (Phillips and Hashash, 2009).

$$G_{NM} = F(G_M - G_{sec}) + G_{min} \quad [6]$$

Here G_M is the Masing shear modulus obtained from the following equation.

$$G_M = \frac{d\tau_M}{d\gamma} \text{ where } \frac{\tau_M - \tau_{rev}}{2} = \frac{G_{max}\left(\frac{\gamma-\gamma_{rev}}{2}\right)}{1+\left(\frac{\gamma-\gamma_{rev}}{2\gamma_r}\right)^{\alpha}} \quad [7]$$

Equation 7 is the unloading/reloading path following the Masing rules, where the backbone curve is shifted to (γ_{rev}, τ_{rev}) and scaled by 2. (γ_{rev}, τ_{rev}) is a point on the backbone curve where an unloading or reloading occurs. G_{sec} is the secant shear modulus equal to τ_{rev}/γ_{rev}. F in equation 6 is a reduction factor to modify G_M to produce a new path in the unloading/reloading. Phillips and Hashash, (2009) introduced F as equation 8 to develop lower damping ratio than induced by the original Masing rules, close to measured data at large strains.

$$F = P_1 - P_2\left(1 - \frac{G_{sec}}{G_{max}}\right)^{P_3} \quad [8]$$

Where P_1, P_2, and P_3 are material constants. The applicability of equation 8 has also been verified by Rollins et al. (2020) to generate damping curves that match experimental data for gravelly soils. G_{min} in equation 6 is responsible for the minimum damping (D_{min}) required at low strains. When $D_{min} = 0$, $G_{min} = G_{sec}$. Yniesta et al. (2017) introduced a shear stress-shear strain relationship for unloading/reloading path by having the damping ratio (D) related to τ_{rev}, and γ_{rev}. If D is equal to D_{min}, then this relationship can be used to calculate G_{min}. Due to the complexity of the formulation, readers are referred to the original study for details.

Figure 2 shows how equation 6 changes the unloading/reloading path from the Masing rules into the non-Masing rules to produce lower damping at large strains and guarantee the presence of minimum damping at low strains.

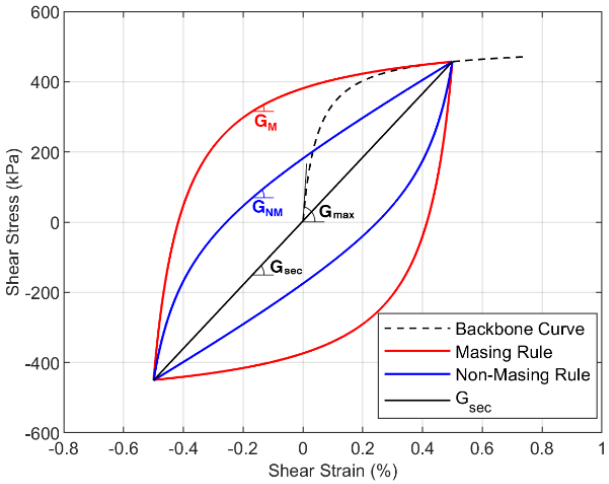

Figure 2 Changes of unloading/reloading path from Masing rules to non-Masing rules using equation 6

By choosing P_1=1, P_2=0, and D_{min}=0, G_{NM} becomes equal to G_M producing identical unloading/reloading path as the Masing rules. Based on the above explanations, the model requires the following material properties:

- to define G_{max}: e, r, A, B
- to define the backbone curve:α, C_u, ϕ, σ_m
- to define damping curve: P1, P2, P3, D_{min}

The presented model is implanted in FLAC 3D as a user-defined model using C++.

3 SEISMIC ANALYSIS OF ROCKFILL DAM

3.1 Dam Geometry and its condition prior seismic loading

The current study performs dynamic numerical analyses of a 90-meter rockfill dam built on hard rock. The dam's geometry and finite difference mesh distribution are illustrated in Figure 3a. The dam's reservoir is assumed to be full, with a 10-meter freeboard. Initial stresses are created through the gravity loading technique before impounding the reservoir. The impoundment is then simulated by applying hydrostatic pressure on the dam's upstream side. For the static conditions, the rockfill behavior is simulated using the Mohr-Coulomb model (i.e. modeling an elastic perfectly plastic stress-strain behavior). Material properties are listed in Table 1. The friction angle and unit weight of the soil are chosen to be representative of the materials used to build earth-fill and rockfill dams, and discussed in the literature (Dakoulas 2012, Razavi et al. 2021). Other material properties are chosen to produce shear wave velocity in the range of 200 to 400 m/s. The generated σ_m, G_{max}, and V_s (shear wave velocity) in the dam axis are shown in Figure 3b.
The element size is defined to permit the propagation of a signal of a maximum frequency of 15 Hz, by restricting the size of the elements to one-tenth to one-eighth of the wavelength (λs) (Itasca 2012). This V_s of the rockfill range from 200 to 400 m/s, resulting in a mesh size of 1.66 m at the crest and 3.33 m at the base. The hydrodynamic pressures on the dam are simulated using the added-mass technique proposed by Zangar (1952).

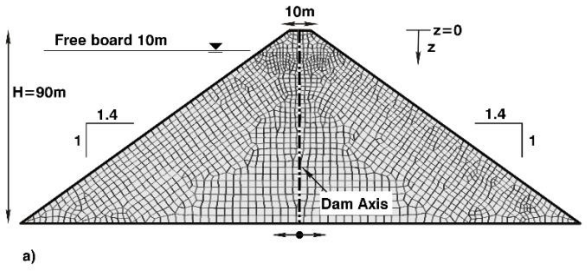

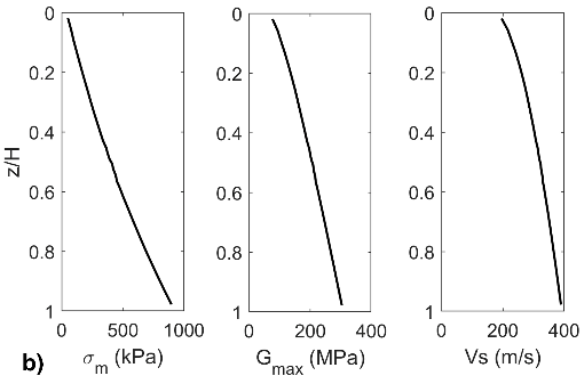

Figure 3 a) Geometry of the rockfill dam, b) variation of σ_m, G_{max}, and V_s with depth at the dam axis

Table 1 material properties of the rockfill

parameters	Value
A	3937.5
B	2.17
r	0.48
e	0.25
Poisson Ratio	0.3
Cohesion	0
Friction Angle	55 degrees
Unit Weight	20 kN/m3

3.2 Seismic Loading

Two input motions are used from the Loma Prieta 1989 earthquake, the LPAND270 record (station number 1652), and the LPGIL067 record (station number 47006). Their acceleration time histories normalized with PGA (peak ground acceleration) and baseline corrected are presented in Figure 4a and Figure 4b. Figure 4c and Figure 4d, present the acceleration response spectra normalized with PGA and the Fourier spectra of the records, respectively. In the present study, these motions are scaled to 0.001g, 0.01g, 0.05g, 0.1g, and 0.2g to investigate the influence of different PGAs on the seismic response of the rockfill dam. Note that the two records differ in their frequency content and duration.

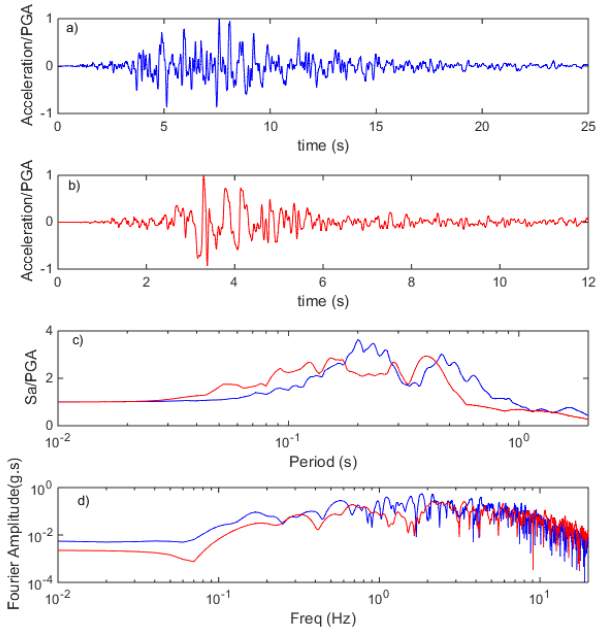

Figure 4 Loma Prieta 1989 earthquake record used: a), acceleration time history of the LPAND270 record (station number 1652), b) acceleration time history of the LPGIL067 record (station number 47006), c) Normalized acceleration response spectra, d) and Fourier spectra of the input earthquakes

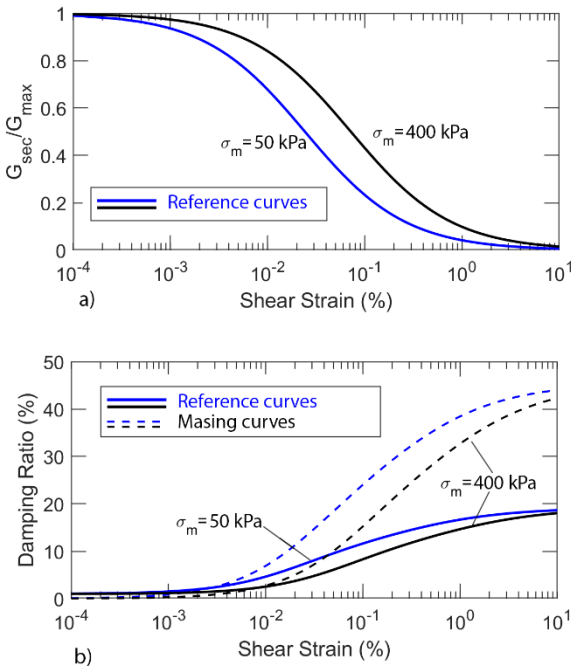

Figure 5 a) Normalized modulus reduction curves, and b) Damping curves obtained using the two sets of parameters presented in Table 2

3.3 Influence of damping curves

In this study the backbone curve of the rockfill is defined using equation 3 with the following material properties : $\alpha = 0.84$, $C_u = 10$, $\phi = 55\ degrees$. Figure 5a shows the normalized shear modulus reduction curve for two confining effective stresses $\sigma_m = 50kPa$ and $\sigma_m = 400\ kPa$. For the damping curves, two different sets of material properties have been selected, and their properties are listed in Table 2. The first set of material properties, labeled Set 1, yields damping curves obtained via the unloading/reloading pathway of the Masing rules. In contrast, the second set of material properties, labeled Set 2 or reference curve, generates material damping curves that closely resemble those suggested by Rollins et al. (2020). The obtained damping curves are shown in Figure 5b.

Table 2 Material damping properties considered in this study

Material Damping parameters	Set 1 Masing curves	Set 2 Reference curves
P1	1	0.6
P2	0	0.2
P3	0	0.9
Dmin (%)	0	1

3.3.1 Results

Figure 6 displays the amplification ratio, defined as the peak acceleration (PA) divided by the input peak ground acceleration (PGA), at various locations along the dam central axis, specifically at z/H=0 (crest), 0.1, 0.33, and 0.75. Here, *z* represents the distance from the crest to the dam's base, while *H* is the total height of the dam. The horizontal axis denotes different levels of PGA at which the input motions were scaled. The results demonstrate that at a low PGA of 0.001g, the amplification ratios of models utilizing the Masing rules get higher than that of non-Masing rules. As the PGA of the earthquake increases the amplification ratios decrease faster for models that use Masing rules. At higher PGA higher strains develop which correspond to the part of the damping curve where the Masing rules significantly overestimate the damping ratio. As the seismic waves are more significantly damped, their intensity decrease leading to a lower amplification.

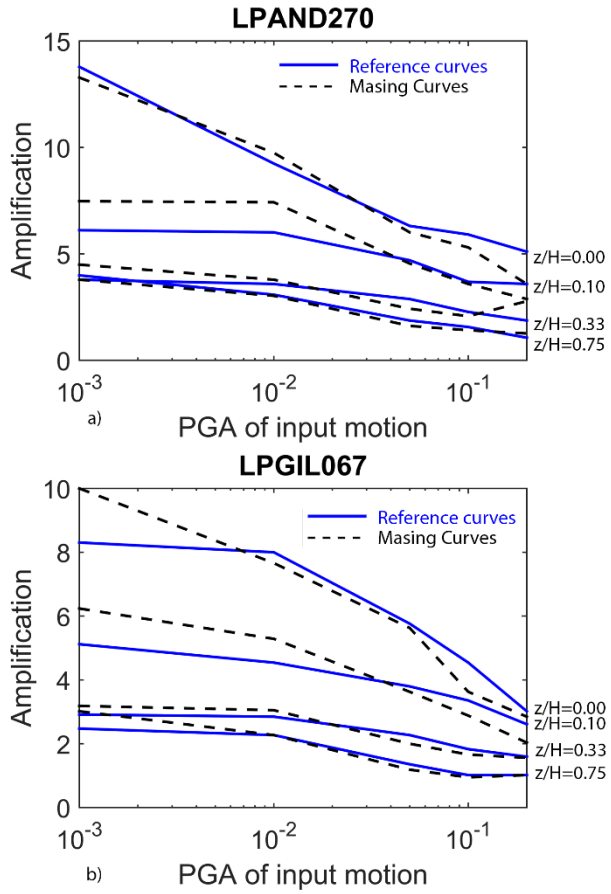

Figure 6 Influence of Masing and Non-Masing rules on the amplification ratio (peak acceleration (PA)/peak ground acceleration (PGA)) at z/H=0, 0.1, 0.33, and 0.75 located at the dam central axis a) for LPAND270 record, b) for LPGIL067 record

3.4 Use of a modified backbone curve

This section introduces a new set of material curves known as the Modified MD curves. These curves do not consider the strength-correction presented in equation 3 but are instead defined by equation 2. The rationale for this decision is that the majority of nonlinear cyclic models available in 2D and 3D software do not offer this option to incorporate the strength-correction factor. These curves follow the Masing unloading/reloading path presented in equation 7, meaning that the MD curves take the Masing properties of set 1 in table 2.

To reduce the high damping observed with the Masing rules (Figure 7b), it is required to modify the backbone curve. Here for example by taking $\alpha = 0.68$ and $\gamma_r = 0.07$, a sample of modified MD curves can be drawn as shown in Figure 7. In the figure the reference curves proposed by Rollins et al. (2020) are also shown. These curves are obtained using the same material properties as in the previous section. The selected modified MD curves exhibit a close match with the curves proposed by Rollins et al. (2020), as can be observed in the figure. However, the drawback of not considering the strength-correction on the backbone curve can be seen in Figure 7c and d, at low and high confining pressure. The higher discrepancy seen at low confining pressures is the results of the input parameters chosen.

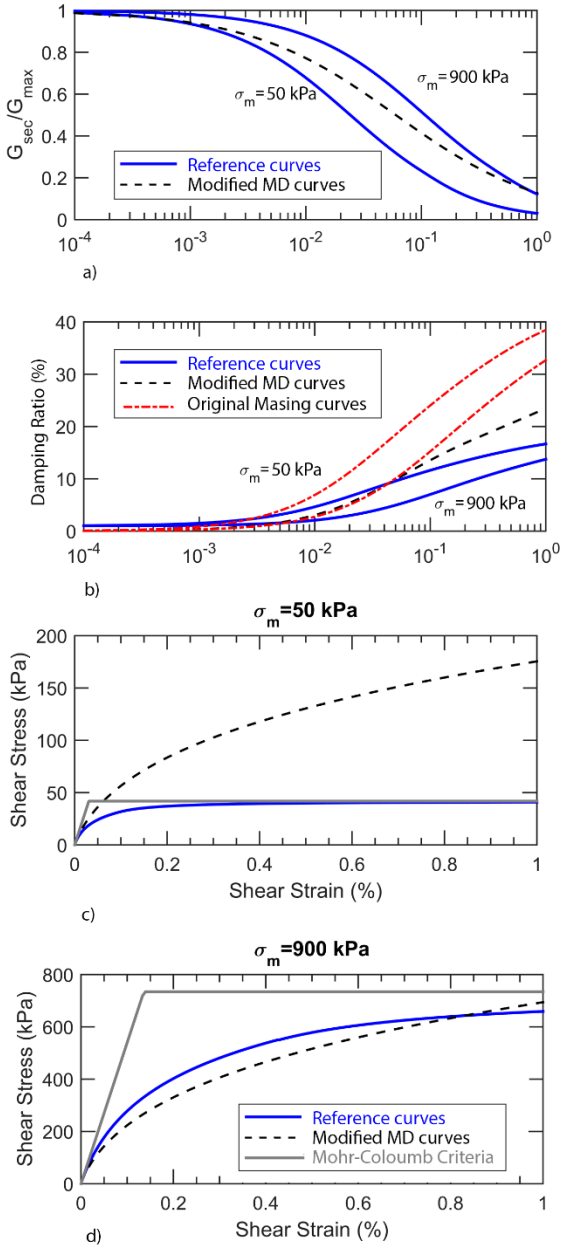

Figure 7 Reference curves versus modified MD curves a) normalized modulus reduction curves, b) damping curves, and c and d) effect of confining pressure on the shape of the backbone curves

3.4.1 Results

As depicted in Figure 7, the modified MD exhibit a near-zero damping ratio. As a result, this approach should use Rayleigh damping to introduce small strain damping. Conversely, at high strains, the curves produce a higher damping ratio. The reduction in stiffness also differs from the lab data and differs at low and high confining pressure. As a consequence of the previous observations, lower amplification values are generally observed when compared to the reference curves. Figure 8 presents the amplification ratio (peak acceleration (PA)/peak ground acceleration (PGA)) at the same locations as previously discussed. However, it should be noted that for the LPGIL067 record the opposite results are observed.

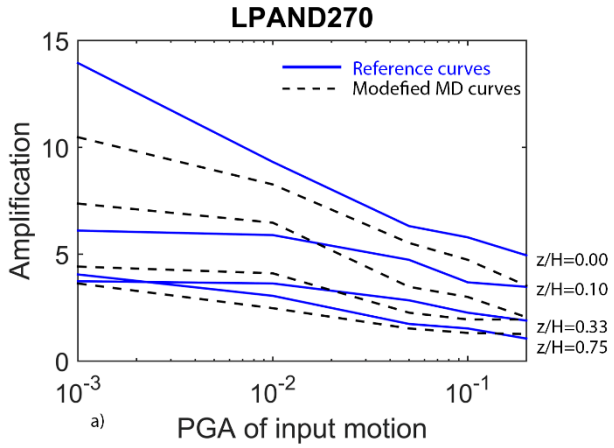

Figure 8 Influence of different approach in the selection of the backbone and damping curves on the amplification ratios (peak acceleration (PA)/peak ground acceleration (PGA)) at z/H=0, 0.1, 0.33, and 0.75 located at the dam central axis for LPAND270 record

4 CONCLUSION

In the present study, a nonlinear cyclic soil model is introduced by combining different approaches from previously published models. The backbone curve is derived from the hyperbolic equation proposed by Konder and Zelasko (1963), with an additional modification suggested by Yee et al. (2013) to reach true shear strength at large strains. The minimum damping is incorporated using the ARCS method introduced by Yniesta et al. (2017), while the remaining damping adheres to the rules established by Phillips and Hashash (2009). As a result, this model combined several features of the previous models and achieve the following goals: (1) no need for viscous damping (Rayleigh damping) at low strains using the coordinate transformation approach of the ARCS model. (2) more accurate damping using non-Masing rules. (3) strength matching at large strains using two hyperbolic curves for backbone curve. (4) confining pressure-dependent curves. The model also has a flexible formulation and the behavior of the nonlinear cyclic models on which it is based can be retrieved by choosing the right input parameters. Using this feature, a parametric study has been done to compare the effect of improvements obtained using the new model on the seismic behavior of a rockfill dam. The following conclusions were made as the results of this study:

- When the same backbone curve is used, the nonlinear cyclic model with higher damping ratio yields lower PGA in the rockfill dam.
- On the other hand, when the backbone curve is modified to have lower damping ratio using Masing rules, the material can become softer and result in reduced PGA. However, the modified curves still maintain high damping ratios at large strains, resulting in lower amplification ratios for strong input motions.

5. REFERENCES

ABAQUS, 2011, Users' Manual, Simulia, Pawtucket, Rhode Island.

Dakoulas, P., 2012. Nonlinear seismic response of tall concrete-faced rockfill dams in narrow canyons. Soil Dynamics and Earthquake Engineering, 34(1), pp.11-24.

Hashash, Y.M., Phillips, C. and Groholski, D.R., 2010, May. Recent advances in non-linear site response analysis. In 5th International Conference on Recent Advances in Geotechnical Earthquake Engineering and Soil Dynamics (No. 4).

Itasca Consulting Group, Inc., 2012. FLAC3D - Fast Lagrangian Analysis of Continua in Three-Dimensions, Ver. 5.0. Software Manual. Minneapolis.

Kondner, R.L. and Zelasko, J. S., 1963. A hyperbolic stressstrain formulation for sands. In Proc. 2nd Pan-American Conf. on SMFE, Sao Paulo, Brazil (Vol. 1, pp. 289-324).

MASING, G., 1926. Eigenspannungen und verfestigung beim messing. In Proceedings, second international congress of applied mechanics (pp. 332-335).

Numanoglu, O.A., Musgrove, M., Harmon, J.A. and Hashash, Y.M., 2018. Generalized non-Masing hysteresis model for cyclic loading. Journal of Geotechnical and Geoenvironmental Engineering, 144(1), p.06017015.

Phillips, C. and Hashash, Y.M., 2009. Damping formulation for nonlinear 1D site response analyses. Soil Dynamics and Earthquake Engineering, 29(7), pp.1143-1158.

Razavi, S.K., Hajialilue-Bonab, M. and Pak, A., 2021. Design of a Plastic Concrete Cutoff Wall as a Remediation Plan for an Earth-Fill Dam Subjected to an Internal Erosion. International Journal of Geomechanics, 21(5), p.04021061.

Richart, F.E., Hall, J.R. and Woods, R.D., 1970. Vibrations of soils and foundations.

Rollins, K.M., Singh, M. and Roy, J., 2020. Simplified Equations for Shear-Modulus Degradation and Damping of

Gravels. Journal of Geotechnical and Geoenvironmental Engineering, 146(9), p.04020076.

Yee, E., Stewart, J.P. and Tokimatsu, K., 2013. Elastic and large-strain nonlinear seismic site response from analysis of vertical array recordings. Journal of Geotechnical and Geoenvironmental Engineering, 139(10), pp.1789-1801.

Yniesta, S., Brandenberg, S.J. and Shafiee, A., 2017. ARCS: A one dimensional nonlinear soil model for ground response analysis. Soil Dynamics and Earthquake Engineering, 102, pp.75-85.

Zangar, C. N. 1952. Hydrodynamic pressures on dams due to horizontal earthquake effects. No. 11. Denver: Technical Information Office.